Proceedings of the ASME 2013 Dynamic Systems and Control Conference
DSCC2013
October 21-23, 2013, Palo Alto, California, USA

DSCC2013-3783

ROBUST DISTURBANCE REJECTION FOR A CLASS OF NONLINEAR SYSTEMS USING DISTURBANCE OBSERVERS

Ahmed H. El-Shaer *
LineStream Technologies
Cleveland, OH
Email: aheshaer@gmail.com

Abdulrahman H. Bajodah
Aeronautical Engineering Department
King Abdulaziz University
Jeddah, Saudi Arabia
Email: abajodah@kau.edu.sa

ABSTRACT

This paper is concerned with disturbance rejection performance in single-input single-output (SISO) nonlinear systems that are described by uncertain linear dynamics and bounded nonlinearities. First, the nonlinear terms are transformed into an equivalent bounded disturbance at the output of a linear system. Then, a disturbance observer (DOB) is added to the closed loop to achieve robust disturbance rejection. The DOB design is formulated as an extended Luenberger observer having internal dynamics with at least an eigenvalue at the origin. The synthesis of a (sub)optimal DOB is carried out by solving multi-objective H_∞ sensitivity optimization. The design approach is applied to an inverted pendulum with actuator backlash. Closed loop response shows that tracking performance is indeed greatly enhanced with the DOB.

1 Introduction

This paper is concerned with disturbance rejection for a class of single-input single-output (SISO) nonlinear systems. The system dynamics is comprised of a linear part subject to norm-bounded uncertainty , and a vector-valued bounded nonlinearity which is not known exactly. Given an internally stabilizing controller which renders the nominal linear dynamics exponentially stable, the nonlinearities can be represented as a bounded disturbance $d(t) \in \mathbb{R}$ at the output of a linear system. A disturbance observer (DOB) is then introduced into the feedback system to eliminate the effect of $d(t)$ in the presence of the linear plant uncertainty.

The main objective in this paper is to enhance performance robustness of a given class of SISO nonlinear feedback systems via linear DOB-based disturbance rejection, using robust control theory [6] [7]. This will be accomplished *without* resorting to any change of coordinates (e.g. local diffeomorphism) to transform the system into the normal form [14] ch. 13. Thus, the approach discussed in this paper applies directly to both matched and mismatched disturbance/uncertainty inputs. It overcomes restrictive relative degree requirements and the necessary matching conditions, revealed by the normal form, which need to be satisfied for disturbance rejection in a large number nonlinear systems see [2] [11] and the references therein.

DOBs are successfully used in many applications including robotics, hard disk drives high-precision servo systems and machine drive tools, see [3] [18] [23]. Moreover, in [20] DOBs are effectively used to suppress the effect of a class of nonlinearities which can be decomposed into a linear part and a bounded nonlinearity. In DOB-based control, an inner loop having a unity-DC gain low pass filter $Q(s)$, is added into the main feedback system to estimate exogenous disturbances and cancel them subsequently [9].

The DOB design presented in this paper relies on the equivalence of the DOB structure in Fig. 1b and that of a classic Luenberger observer state estimation of an augmented linear system with internal model for the disturbance dynamics [13]. Under mild assumptions it is shown that such equivalence indeed exists if the internal model has at least an eigenvalue at the origin [18]. Thus, once the Luenberger observer gain L is obtained, $Q(s)$ is evaluated as a transfer function parameterized by the gain L, i.e. $Q(s,L)$. This approach offers many advantages over conventional methods [23], which include: (i) the design of DOBs is systematically embedded into the more general framework of robust state estimation of uncertain [10] and nonlinear systems [11], (ii) the design of the inner DOB and an outer

*Address all correspondence to this author.

controller can be carried out completely separately, (iii) structure constraints associated the $Q(s)$ filter (e.g. the DC constraint $Q(0)=0$) are readily satisfied in the new design, (iv) additional frequency shaping can be transparently introduced into the DOB by incorporating appropriate disturbance modes in the internal model dynamics. Thus, the DOB filter $Q(s)$ can be designed with more flexibility in regards to its order, bandwidth and roll-off rate. Hence, disturbance rejection performance is greatly enhanced and robustness of the overall system is achieved.

The DOB synthesis is then formulated as a constrained H_∞ sensitivity optimization which can be efficiently solved for a local (sub)optimal observer gain in a number of ways including semi-definite programming [9], nonlinear programming [15] [16] and non-smooth H_∞ synthesis [1] [12]. Finally, the design approach is applied to a nonlinear inverted pendulum with input backlash nonlinearity. Simulation results indicate that DOB-based control achieves robust tracking and disturbance rejection of the closed loop system.

2 Problem Statement

This paper is concerned with the SISO nonlinear system

$$\begin{aligned} \dot{x} &= Ax + Bu + g(x,u) \\ y &= Cx, \end{aligned} \tag{1}$$

where $x(t) \in \mathbb{R}^n$, $u(t), y(t) \in \mathbb{R}$, and $g : \mathbb{R}^n \times \mathbb{R} \to \mathbb{R}^n$ is vector-valued nonlinearity collecting nonlinear terms in the plant and actuator. It is assumed that the functional form of $g(.,.)$ *is not exactly known*, however the map $t \mapsto g(x(t),u(t)) \in L_\infty^n$; that is

$$\|g\|_\infty := \max_{1\le i\le n} \sup_{\chi(t)\in\mathbb{R}^{n+1}} \sup_{t\ge 0} |g_i(x(t),u(t))| \le m_g < \infty, \tag{2}$$

where $\chi(t) := \begin{bmatrix} x(t)^T & u(t) \end{bmatrix}^T$. The assumption (2) is satisfied by many nonlinearities arising in dynamical systems such as flexible-joint robots [22], certain chaotic systems [21] as well as classes hysteresis operators [10]. More generally, $g(.,.)$ can represent an unknown norm-bounded perturbation acting on a linearized system, see [14] ch. 9. Furthermore, the transfer function $P(s) = C(sI-A)^{-1}B$ satisfies the multiplicative uncertainty

$$P(s) = P_n(s)(1+\Delta(s)),\ \Delta(s) \text{ stable}, \|\Delta\|_\infty \le 1, \tag{3}$$

where $\|\,.\,\|_\infty$ is the H_∞ norm [4] [6] [7], and $P_n(s) = C_p(sI-A_p)^{-1}B_p$ is the nominal transfer function. Hence, the nominal nonlinear system is

$$\begin{aligned} \dot{x}_p &= A_p x_p + B_p u + g(x_p,u) \\ y_p &= C_p x_p. \end{aligned} \tag{4}$$

The following assumptions are made

(A1) The nominal plant $P_n(s)$ is minimum phase,
(A2) The pair (A_p, C_p) is detectable.

Let $K(s)$, given in (5), be an internally stabilizing controller, designed *a priori* to achieve good tracking performance for $P_n(s)$

$$\begin{aligned} \dot{x}_k &= A_k x_k + B_k e \\ u &= C_k x_k + D_k e \end{aligned} \tag{5}$$

where $x_k(t) \in \mathbb{R}^{n_k}$, $e(t) = y_{ref}(t) - y_p(t)$ is the nominal tracking error, and $y_{ref}(t) \in \mathbb{R}$ is a bounded reference input. From (4) and (5), the output y_p of the nominal closed loop system is given by

$$\begin{aligned} y_p(t) = &\underbrace{C_{cl}\left[e^{A_{cl}t}x_{cl}(0) + \int_0^t e^{A_{cl}s}\begin{bmatrix} B_pD_k \\ B_k \end{bmatrix} y_{ref}(t-s)\,ds\right]}_{y_{nom}(t)} + \\ &\underbrace{C_{cl}\int_0^t e^{A_{cl}s} g_{cl}(x_{cl})(t-s))\,ds}_{y_{pert}(t)}, \end{aligned} \tag{6}$$

where $x_{cl} = \begin{bmatrix} x_p \\ x_k \end{bmatrix}$, $C_{cl} = \begin{bmatrix} C_p & 0 \end{bmatrix}$, $g_{cl}(x_{cl})(t) = \begin{bmatrix} g(x_p, C_k x_k + D_k e)(t) \\ 0 \end{bmatrix}$ and $A_{cl} = \begin{bmatrix} A_p - B_p D_k C_p & B_p C_k \\ -B_k C_p & A_k \end{bmatrix}$. Hence, (6) is rewritten as

$$y_p(t) = y_{nom}(t) + y_{pert}(t),$$

where y_{nom} denotes the response of the nominal linear dynamics and y_{pert} is a perturbation term accounting for $g(.,.)$. Define

$$d(t) := y_{pert}(t) = C_{cl}\int_0^t e^{A_{cl}s} g_{cl}(x_{cl})(t-s))\,ds, \tag{7}$$

by virtue of internal stability (i.e. A_{cl} is Hurwitz), there exist $k > 0$ and $\alpha > 0$ such that $\|e^{A_{cl}t}\| \le ke^{-\alpha t}$ [5] p. 59. Consequently,

$$\|d(t)\| \le k\|C_{cl}\|_\infty \int_0^t e^{-\alpha\theta}\|g(x_{cl})(t-\theta)\|\,d\theta \le \frac{k\|C_{cl}\|_\infty m_g}{\alpha}. \tag{8}$$

Thus, d is a norm-bounded exogenous disturbance at the output y_p. In the presence of $\Delta(s)$, exponential stability of the underlying linear closed loop dynamics (i.e. (1) with $g(.,.) \equiv 0$), is sufficient for $d(t)$ to be uniformly bounded, which will be established in the next section using the small gain theorem. This motivates the use of a disturbance observer (DOB) to achieve robust closed loop tracking performance by rejecting potentially degrading effects of the disturbance $d(t)$ so that the closed loop recovers nominal linear behavior for all $\Delta(s)$ satisfying (3). It is also noted that the construction in this section includes both *matched and mismatched* nonlinearities.

3 Disturbance Observers

3.1 Overview

As shown in Fig. 1, the DOB introduces an inner loop into the feedback system where $Q(s)$ is a *stable unity DC gain low pass filter* with *desired bandwidth*, and is considered the design parameter. DOB-based control is studied in more details in [18] and in El-Shaer et.al. [9]. In Fig. 1a, d captures the effect of the nonlinearities $g(.,.)$ in the plant/actuator dynamics. The primary objective of the DOB is to produce an estimate $\hat{w}$ and *feed it*

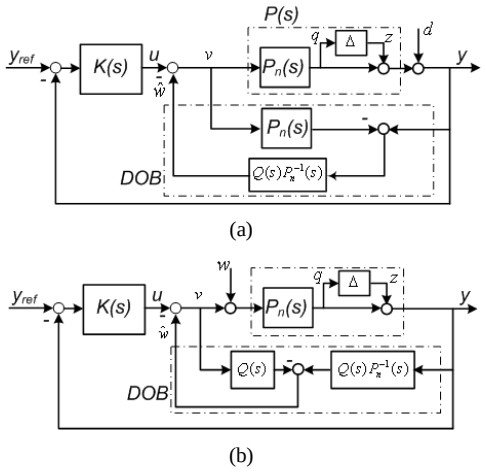

Figure 1. DOB-based closed loop system: (a) The exogenous disturbance d at the output, (b) equivalent DOB structure with exogenous disturbance w at the input

back to the nominal control input u to cancel the effect of d. It is important to note that $\hat{w}$ represents the equivalent estimate of d reflected at the plant's control input. From Fig. 1a

$$\begin{aligned} &\hat{w} = Q(s)P_n^{-1}(s)(y - P_n(s)v) \\ &\implies \hat{w} = Q(s)P_n^{-1}y - Q(s)v. \end{aligned} \tag{9}$$

Thus, the DOB scheme in Fig. 1a is equivalent to that in Fig. 1b, with the latter regarded as rejection of an exogenous disturbance w at the input of $P(s)$. It is noted that $Q(s)P_n^{-1}$ is stable by assumption (A1). In the sequel, the DOB structure in Fig. 1b is shown to be equivalent to a Luenberger observer of an augmented dynamical system. This renders the design of optimal DOB more systematic and overcomes structural constraints associated the filter $Q(s)$. Hence, the DOB configuration in Fig. 1b is used in the analysis hereafter.

3.2 Robust Disturbance Rejection

From Fig. 1b, assuming that $P_n(s) = P(s)$, the output $y = y_p$ is given by

$$y = \frac{P_n(s)K(s)y_{ref} + P_n(s)(1-Q(s))w}{1 + P_n(s)K(s)}. \tag{10}$$

The following closed loop sensitivity functions are defined

$$S(s) = \frac{P_n(s)(1-Q(s))}{1+P_n(s)K(s)}, \; T(s) = \frac{P_n(s)K(s)+Q(s)}{1+P_n(s)K(s)} \tag{11}$$

From Fig. 1b, $S(s) = -G_{w\to e}(s)$ where e is the tracking error, and $T(s) = -G_{z\to q}(s)$ where z and q are the interconnection variables of the nominal closed loop system and the uncertainty $\Delta(s)$ (see Fig. 1). Eq. (11) indicates that further reduction in $S(s)$ is achieved by having $Q(s) = 1$ over a desired frequency band.

Robust stability of the closed loop systems in Figs. 1a and 1b is equivalent to that of Fig. 2. Suppose, for a given stable

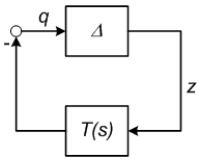

Figure 2. Robust stability analysis.

$Q(s)$ that $T(s)$ is exponentially stable, and let $W_u(s)$ be a stable weighting function such that $|\Delta(j\omega)| \le |W_u(j\omega)| \; \forall\, \omega$ and $\Delta(s)$. Then, the *small gain* condition [6] [7]

$$\|W_u T\|_\infty < 1 \tag{12}$$

guarantees that the closed loop in Fig. 2 is (internally) exponentially stable $\forall \Delta(s)$ in (3). Therefore $d(t)$ in Fig. 1a is L_∞-bounded signal, hence also $\hat{w} \in L_\infty$. Also, note that $G_{w\to\hat{w}}(s) = Q(s)$. Thus, given a stable weighting function $W_p(s)$, then

$$\begin{aligned} &\|W_p(1-Q)\|_\infty \le \gamma \\ &\implies \|W_p(w-\hat{w})\|_{L_2} \le \gamma \|w\|_{L_2}, \end{aligned} \tag{13}$$

where $\gamma > 0$ is a given performance bound and $w - \hat{w}$ is the disturbance estimation error (Fig. 1b). Hence, (12) and (13) guarantee robust disturbance rejection. Also $\|W_p(1-Q)\|_\infty \le \gamma$ sets a lower bound on the cut-off frequency of the high pass filter $1 - Q(s)$. Thus, $W_p(s)$ can be selected to set desired bandwidth for $Q(s)$. The conditions (12) and (13) will be used in the sequel to formulate a multi-objective H_∞ optimization for the DOB synthesis.

3.3 Q Filter Design

The low pass filter $Q(s)$ is typically given by [3] [18] [9] [23]

$$Q(s) = \frac{1 + \sum_{k=1}^{m-\rho} a_k (\tau s)^k}{1 + \sum_{k=1}^{m} a_k (\tau s)^k} \tag{14}$$

where $m > 0$ is the order of $Q(s)$ and $\rho \le m$ is its relative degree. The design trade-off of $Q(s)$ is to choose $\{a_k\}_{k=1}^m \ge 0$ such that its cut-off frequency $\omega_c \approx 1/\tau$ is large enough for better disturbance rejection. However, a direct synthesis of $Q(s)$ in (14) is subject to

(Q1) *Relative degree*: ρ must be greater than or equal the relative degree of $P_n(s)$ to make $Q(s)P_n^{-1}(s)$ realizable,
(Q2) *Unity DC gain*: $Q(0) = 1$ imposes that ρ and $\{a_k\}_{k=1}^m$ are not independent of each other [23],
(Q3) Robust stability of the closed loop system (i.e. (12)).

These constraints complicate the synthesis of an optimal $Q(s)$. Thus, an alternative design method is sought where the structure requirements (Q1) and (Q2) are implicitly satisfied to ease the complexity of the synthesis process.

3.4 Internal Model-based Luenberger Observer

In this section, robust disturbance estimation is formulated as the design of a Luenberger observer for an augmented system with an internal model of the disturbance. It is shown that the DOB-based disturbance estimation given in Fig. 1b is equivalent to that based on the Luenberger observer. Consequently, $Q(s)$ satisfying (Q1), (Q2) and (Q3) is parameterized by the Luenberger observer gain which can be systematically designed via a multi-objective H_∞ sensitivity optimization.

The analysis below is concerned with a general exogenous disturbance $w(t)$ which is not necessarily the same as the effect of the nonlinearity $d(t)$ (7) reflected at the input of the plant as in Fig. 1b, see Remark 2 below. Suppose the disturbance $w(t)$ is generated by the linear exo-system [13]

$$\begin{aligned} \dot{x}_w = A_w x_w, \quad x_w(t_0) = x_{w0} \\ w = C_w x_w, \end{aligned} \tag{15}$$

where $x_w(t) \in \mathbb{R}^{n_w}$. The state space representation in (15) is assumed to satisfy

(A3) The pair (A_w, C_w) is detectable,
(A4) The eigenvalues of A_w don't coincide with the zeros of the plant $P_n(s)$, which implies that the disturbance state x_w is observable from the output y_p.

Define $\tilde{x} = \begin{bmatrix} x_p^T & x_w^T \end{bmatrix}^T$, the augmented system, comprised of the nominal plant and the exo-system, is given by (see Fig. 3)

$$\dot{\tilde{x}} = \tilde{A}\tilde{x} + \tilde{B}v, \quad \tilde{y} = \tilde{C}\tilde{x} \tag{16a}$$

$$\tilde{A} = \begin{bmatrix} A_p & B_p C_w \\ 0 & A_w \end{bmatrix}, \tilde{B} = \begin{bmatrix} B_p \\ 0 \end{bmatrix}, \tilde{C} = \begin{bmatrix} C_p & 0 \end{bmatrix} \tag{16b}$$

Given assumptions (A2), (A3) and (A4), it can be shown that

$$rank \left(\begin{bmatrix} \lambda I - \tilde{A} \\ \tilde{C} \end{bmatrix} = \begin{bmatrix} \lambda I - A_p & -B_p C_w \\ 0 & \lambda I - A_w \\ C_p & 0 \end{bmatrix} \right) = n_p + n_w \tag{17}$$

for all eigenvalues $\lambda \in \mathbb{C}$ of $\tilde{A}$. From the PBH observability rank condition [7] p. 82, the augmented system in (16) is detectable, see [9] [22]. Hence, there exists $L \in \mathbb{R}^{n_p + n_w}$ such that

$$\dot{\hat{x}} = \left(\tilde{A} - L\tilde{C}\right)\hat{x} + \begin{bmatrix} \tilde{B} & L \end{bmatrix} \begin{bmatrix} v \\ y_p \end{bmatrix} \tag{18}$$

is an asymptotically stable extended state observer for the system (16). Moreover, using the coordinate transformation $T = \begin{bmatrix} I & 0 & 0 & 0 \\ 0 & I & 0 & 0 \\ I & 0 & I & 0 \\ 0 & 0 & 0 & I \end{bmatrix} \left(\in \mathbb{R}^{2n_p + n_k + n_w}\right)$, the eigenvalues of the overall closed loop system, comprised of $P_n(s)$, $C(s)$ and the Luenberger observer (18), can be decomposed as follows

$$\begin{aligned} \det(\lambda I - T^{-1} \begin{bmatrix} A_p - B_p D_k C_p & B_p C_k & 0 & -B_p C_w \\ -B_k C_p & A_k & 0 & 0 \\ L_1 C_p - B_p D_k C_p & B_p C_k & A_p - L_1 C_p & 0 \\ L_2 C_p & 0 & -L_2 C_p & A_w \end{bmatrix} T) \\ = \det(\lambda I - A_{cl}) \ \det\left(\lambda I - \left(\tilde{A} - L\tilde{C}\right)\right), \end{aligned} \tag{19}$$

where A_{cl} is given in (6), $\tilde{A} - L\tilde{C} = \begin{bmatrix} A_p - L_1 C_p & B_p C_w \\ -L_2 C_p & A_w \end{bmatrix}$ and $L = \begin{bmatrix} L_1^T & L_2^T \end{bmatrix}^T$ with $L_1 \in \mathbb{R}^{n_p}$ and $L_2 \in \mathbb{R}^{n_w}$. Thus, closed loop exponential stability is achieved if and only if each of A_{cl} and $\tilde{A} - L\tilde{C}$ is Hurwitz. This clearly allows $K(s)$ to be designed separately of the state estimator.

3.5 Equivalence to the DOB

The 2 methods considered for disturbance estimation, depicted in Fig. 3, are summarized as follows

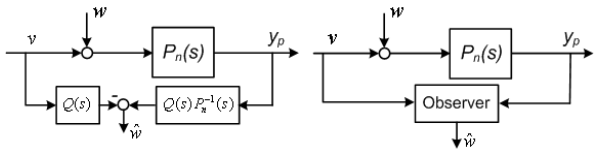

Figure 3. Disturbance estimation: DOB (left), observer based (right)

1. *Observer-based*: from (18) and Fig. 3, the estimate $\hat{w}$ is given by

$$\begin{aligned} \hat{w} = -G_1(s)v + G_2(s)y_p \\ \begin{bmatrix} G_1(s) \\ G_2(s) \end{bmatrix} = \tilde{C}_w \left(sI - \left(\tilde{A} - L\tilde{C}\right)\right)^{-1} \begin{bmatrix} -\tilde{B} \\ L \end{bmatrix}, \end{aligned} \tag{20}$$

   $\tilde{C}_w = \begin{bmatrix} 0 & C_w \end{bmatrix}$.
2. *DOB-based*: from (9), the estimate $\hat{w}$ is given by

$$\hat{w} = -Q(s)v + Q(s)P_n^{-1}(s)y_p. \tag{21}$$

The equivalence between the *DOB-based* estimate in (21) and the *observer-based* estimate in (20) is stated next.

Theorem 1: Suppose that assumptions (A2), (A3) and (A4) are satisfied, and that A_w has at least one of its eigenvalues at the origin. Then the expressions in (20) and (21) for $\hat{w}$ are equivalent; that is, $Q(s) = G_1(s)$ and $Q(s)P_n^{-1}(s) = G_2(s)$. In particular, $Q(0) = G_1(0) = 1$.
Proof: Details in [18] pp. 543–546 ☒.

In particular, $G_1(s)$ is a *low-pass filter with unity DC gain*, and $Q(s)P_n^{-1}(s) = G_2(s)$ is indeed realizable. Hence, the unity DC gain (Q1) and the the relative degree (Q2) constraints hold. Once L is obtained, $Q(s)$ is evaluated using $G_1(s)$ in (20). Hence, from Theorem 1 it follows that a Luenberger observer with sufficiently large bandwidth (i.e. eigenvalue placement for $\tilde{A} - L\tilde{C}$), allows the DOB-based estimate $\hat{w}$ (21) to asymptotically track any w given by (15); that is

$$\lim_{t \to \infty} (w(t) - \hat{w}(t)) = 0. \tag{22}$$

Together with (13) and (12), robust asymptotic disturbance estimation and rejection are indeed achieved.

Remark 1: Some advantages of this approach are: (i) the structure constraints (Q1) and (Q2) are satisfied, (ii) internal stability of the nominal closed loop system is guaranteed by virtue of (19), and (iii) a wide variety of exogenous disturbances can be transparently accommodated into this design by incorporating their signal models in A_w (see (23)).

Remark 2: It must be emphasized that $d(t)$ resulting from the nonlinearity $g(.,.)$ (7), *is not* generated by (15) which serves as a fictitious augmented state to ensure that $Q(s)$ satisfies (Q1) and (Q2). This enables DOB-based controllers to reject signals not having well defined spectral content. Accommodating disturbances other than $d(t)$ (7) is readily done by expressing $w(t)$ in (15) as

$$\begin{aligned} w(t) &= A_1 w_1(t) + A_2 w_2(t) \\ W_1(s) &= \tfrac{1}{s^{n_{w1}}},\ W_2(s) = \tfrac{n_{W_2}(s)}{d_{W_2}(s)}, \end{aligned} \tag{23}$$

where $w_1(t)$ ensures that A_w has at least one eigenvalue at the origin. In particular, different choices of $d_{W_2}(s)$ allows the signal $w_2(t)$ to model a wide variety of exogenous disturbances. Moreover, the amplitudes A_1 and A_2 are scaling factors to reduce measurement noise amplification, also when $A_2 \equiv 0$ the so-called proportional-integral (PI) Luenberger observer is recovered, see [22].

4 Synthesis Optimization

From (12), (13) and (20), an optimal $Q(s)$ can be synthesized from the following constrained H_∞ sensitivity optimization

$$\min_{L \in \mathbb{R}^{n_p+n_w}} \|W_p(s)(1-Q(s,L))\|_\infty \tag{24a}$$

subject to:

$$\|W_u(s)T(s,L)\|_\infty < 1, \tag{24b}$$

$$\left\|W_p(s)(1-Q(s,L))\right\|_\infty \le \gamma, \tag{24c}$$

$$\max_i Re\{\lambda_i\{\tilde{A}-L\tilde{C}\}\} \le -\sigma_S \tag{24d}$$

where $Q(s,L) = G_1(s)$, and $T(s,L)$ is given by (11), $\gamma > 0$ and $\sigma_S > 0$ are fixed performance and stability bounds, respectively. The inequality (24d), ensures that $\tilde{A}-L\tilde{C}$ is Hurwitz with $-\sigma_S$ guaranteed decay rate. For practical purposes, the objective and/or constraints given above are usually restricted to problem-specific finite frequency intervals reflecting desired performance. The expressions (24) involve the non-smooth H_∞-norm, and are non-convex in L.

In El-Shaer et. al. [9] and [10], the synthesis (24) is expressed as the weighted sensitivity optimization:

$$\min_L \gamma \quad \text{subject to: } \left\| \begin{bmatrix} W_u T \\ W_p(1-Q) \end{bmatrix} \right\|_\infty \le \gamma,\ \gamma < 1,$$

which is then turned into rank-constrained semi-definite program (SDP) [7] p. 231, for a static output feedback (sub)optimal gain L. However, the solution obtained is too conservative since both robust stability (24b) and robust performance (24c) are expressed by a single Lyapunov SDP variable, see [9] for details. Alternatively, parametric optimization over L using nonlinear programming (NLP) gives freedom to optimize individual performance constraint bounds, at the expense of non-smooth cost and constraint functions.

Given an initial observer gain L_0, a local (sub)optimal L of (24) can be obtained using subgradient-based non-smooth H_∞ synthesis of fixed-structure controllers presented in [1]. Currently, this algorithm solves sensitivity minimization with no eigenvalue-placement constraints, i.e. unconstrained single or multiple sensitivity problems [12]. However, for the more general setting (e.g. (24)), finite difference approximation of the gradients allows available powerful interior-point NLP algorithms to handle multi-objective H_∞-synthesis constraints, see [16] ch. 19 and [15].

5 Simulation Example

The rotation dynamics of a fixed-based inverted pendulum about the vertically upright equilibrium position (i.e. $\theta = 0$, $\dot{\theta} = 0$) is

$$\begin{aligned} ml^2\ddot{\theta} + b\dot{\theta} + k\theta &= mgl\sin(\theta) + T_{in}(v) + T_{dist}; \\ m = 0.25\,[kg],\ l = 0.5\,[m],\ b &= 0.001\,[N.m.sec], \\ k = 0.1\,[N.m],\ g &= 9.81[m/sec^2]. \end{aligned} \tag{25}$$

In (25), $T_{in} = N(v)\ [N.m]$ is the input torque, v is the (total) control signal (see (32)) and $N(.)$ is backlash nonlinearity in the drive shaft and $T_{dist}\ [N.m]$ represents disturbance torques described below.

The presence of backlash is known to cause limit cycle oscillations in closed loop systems [17]. The graph of a non-symmetric backlash nonlinearity in displayed in Fig. 4, where the slopes m_1, m_2 and K_N are finite, and the dead-band width is given by $\Delta_1 - \Delta_2$, see [17] [8] [19]. An exact analytic form of $N(.)$ might be too complicated and is not needed for robust DOB design. In fact, the output of $N(v)(t)$ can be written as [19] [20]

$$T_{in}(v) = N(v)(t) = K_N v(t) + \eta(t), \tag{26}$$

where $\eta(t)$ is a nonlinearity such that

$$\begin{aligned} \|\eta\|_\infty = \sup_{t\ge 0}|\eta(t)| \le \max\{ &\sup_{v(t)\in\mathbb{R}}(m_+(v) - K_N v), \\ &\sup_{v(t)\in\mathbb{R}}(K_N v - m_-(v))\}. \end{aligned} \tag{27}$$

In (27), $m_+(.)$ and $m_-(.)$ are piecewise continuous curves such that

$$m_-(v(t)) \le N(v)(t) \le m_+(v(t)),\ \forall t \ge 0,\ v \in L_\infty. \tag{28}$$

Given K_N, the choices $m_+(v) := K_N v + n_v$ and $m_-(v) := K_N v - n_v$, establish that the smallest value n_v which intercepts the $N(.)$-axis is a bound on $\|\eta\|_\infty$, see Fig. 4. Thus, η is indeed norm bounded. The state space representation of (25) is given by

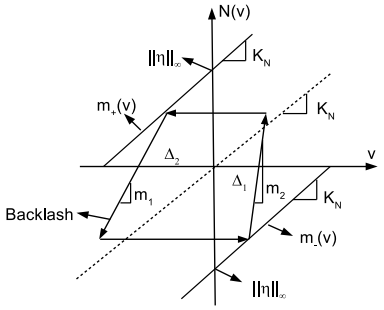

Figure 4. Graph of the backlash $N(.)$

$$\dot{x} = \begin{bmatrix} 0 & 1 \\ \frac{-k}{ml^2} & \frac{-b}{ml^2} \end{bmatrix} x + \begin{bmatrix} 0 \\ \frac{K_N}{ml^2} \end{bmatrix} v + \begin{bmatrix} 0 \\ \frac{g\sin(x_1)}{l} + \frac{\eta(t)}{ml^2} \end{bmatrix} + \begin{bmatrix} 0 \\ \frac{1}{ml^2} \end{bmatrix} T_{dist}$$
$$y = \begin{bmatrix} 1 & 0 \end{bmatrix} x \tag{29}$$

which is the same as (1) with the additional term T_{dist}.

The slope K_N is assumed to be given by $K_N = \bar{K}_N + r_K\delta_K$; $\bar{K}_N = 1$, $r_K = 0.75$ and $|\delta_K| \le 1$. From (25), the uncertain and nominal plant dynamics are given by

$$P(s) = \frac{K_N}{ml^2s^2 + bs + k},\ P_n(s) = \frac{\bar{K}_N}{ml^2s^2 + bs + k}. \tag{30}$$

Hence, from (3)

$$W_u(j\omega) = \frac{|P(j\omega) - P_n(j\omega)|}{|P_n(j\omega)|} \le r_K. \tag{31}$$

In (29), the nonlinearity $\sin(x_1)$ is fully known since the measured output $y = x_1$. This motivates the following control law

$$v = -\frac{ml\,g\sin(x_1)}{\bar{K}_N} + u, \tag{32}$$

where $u = K(s)[y_{ref} - y]$, see Fig. 1. The outer controller, designed for $P_n(s)$, is chosen as a simple lead compensator

$$K(s) = 5\frac{2.5s+1}{0.25s+1}. \tag{33}$$

The expression (32) is comprised of: (i) feedback linearization to cancel the nonlinearity $\sin(x_1)$, and (ii) tracking error compensation based on $K(s)$. Thus, the objective of the DOB is to reject the effects of T_{dist} and the norm-bounded nonlinear uncertainty $\eta(t)$.

Let T_{dist} represent structure vibration modeled as lightly damped sinusoid at ω_w. From (29), the total disturbance (23) is given by

$$w(t) = \eta(t) + T_{dist}(t), \tag{34}$$

and the disturbance dynamics

$$W_1(s) = \frac{1}{s}, \quad W_2(s) = \frac{\omega_w^2}{s^2 + 2\zeta\omega_w s + \omega_w^2}, \tag{35}$$

where $\zeta = 0.002$, $\omega_w = 5(2\pi)$ $[rad/sec]$. Hence, the exo-system (15) is

$$A_w = \begin{bmatrix} 0 & 0 & 0 \\ 0 & 1 & 0 \\ 0 & -\omega_w^2 & -2\zeta\omega_w \end{bmatrix},\ C_w = \begin{bmatrix} A_1 & A_2 & 0 \end{bmatrix};\ A_1 = 100, A_2 = 500. \tag{36}$$

It is easily verified that the conditions in Theorem 1 are satisfied. The weighting function $W_p(s)$ is chosen as

$$W_p(s) = 0.5\frac{s+2(2\pi)}{s+0.5}\,\frac{s^2 + 2(0.8\zeta)\omega_w s + \omega_w^2}{s^2 + 2(1.5\zeta)\omega_w s + \omega_w^2}, \tag{37}$$

which has a resonant mode at ω_w and specifies at least 8 Hz cut-off frequency for $Q(s)$. Eigenvalue placement for $\tilde{A}$ at $\{-8,-12,-18,-24,-34\}$ yields $L_0 = [154.62, 5.99, 0.893, -4.648, -245.985]^T$.

5.1 Optimization Results

For $\sigma_S = 8$ and $\gamma = 2$, the NLP (24) is specialized to

$$\min_{L\in\mathbb{R}^5} \max_{\omega\in(2\pi)\times[0.1,8]} \left|W_p(j\omega)(1 - Q(j\omega, L))\right|,$$
$$\text{subject to: (24b), (24c), (24d),} \tag{38}$$

which confines the objective (24a) to the frequency range $\omega \in (2\pi)\times[0.1,\ 8]$ $[rad/sec]$. The synthesis (38) is solved using the interior point solver within the `fmincon` command in the Optimization Toolbox of Matlab Version 7.14 (R2012b), which implements a trust region-based sequential quadratic programming (SQP), see [15] [16] and the references therein[1]. In particular, the H_∞-norm of the transfer functions involved in (38) is evaluated using the algorithm presented in [4][2]. Convergence takes place after 60 iterations to $L = [1561.3, 15.174, 121.18, 144.91, -163.2]$ with objective function value $\max_{\omega\in(2\pi)\times[0.1,8]} \left|W_p(j\omega)(1 - Q(j\omega, L))\right| = 0.36$, see Fig. 5.

Table 1 shows the solution for (24) using NLP, the iterative SDP algorithm in [9] and the non-smooth synthesis [1] which is implemented in `hinfstruct` in the Robust Control Toolbox, Matlab (R2012b) [12]. From Table 1, the robust stability condition $\|W_u T\|_\infty < 1$ is satisfied only by the NLP-based solution (i.e. with `fmincon`), which will be used below for closed loop simulation.

From (20) the DOB filter is

$$Q(s) = \frac{1.353\times10^6 s^2 - 1.136\times10^6 s + 1.914\times10^8}{s^5 + 242.9s^4 + 2.6\times10^4 s^3 + 1.596\times10^6 s^2 + 2.353\times10^7 s + 1.914\times10^8}, \tag{39}$$

which is stable unity-DC gain with cut-off frequency at 13 Hz. Although $Q(s)$ turned out non-minimum phase, the product $Q(s)P_n^{-1}(s)$ is stable as required for the stability of the feedback system depicted in Fig. 1. As shown in Fig. 6, $Q(s)$ satisfies the robust performance bound (24c) $\|W_p(1-Q)\|_\infty = 1.48 < \gamma = 2$. Also, $\|W_u T\|_\infty = 0.987 < 1$ as required by the robust stability condition (24b).

[1] Central difference is chosen to approximate gradients with relative perturbation 1×10^{-6} and BFGS for Hessian matrix updates.

[2] The function `norm` in the Matlab Control Toolbox.

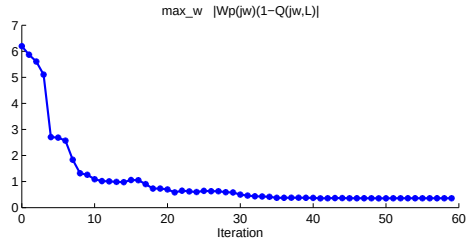

Figure 5. Evolution of the objective function

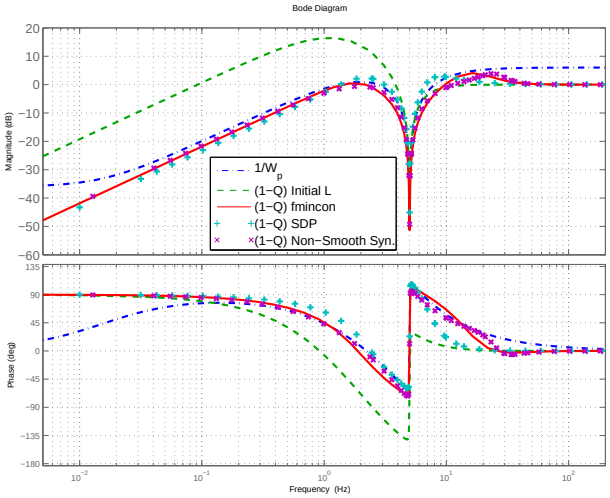

Figure 6. Bode plots of $1/W_p(s)$ (dash-dot), $1-Q(s)$; initial L (dash), optimized L (solid)

5.2 Simulation Results

All simulations are carried out in Simulink Version 7.9 (R2012b) for the closed loop comprised of the nonlinear system (25) with the controller (32) and DOB inner loop having $Q(s)$ (39). In both cases below, the tracking error $e = y_{ref} - y$ is obtained for the reference input $y_{ref}(t) = \frac{\pi}{3}\sin(2\pi f t)$; $f = \frac{3}{4}\,Hz$ and *in the presence* of the disturbance torque $T_{dist}(t) = \sin(\omega_w t)$; $\omega_w = 5(2\pi)\,[rad/sec]$.

5.2.1 Case I: Inverted Pendulum without Backlash

In the first simulation, the backlash nonlinearity is taken out; that is, $T(u) = u$ in (25). The closed loop response is shown in Figs. 7 and 8. The rms values of the tracking error are 0.0482 and 0.0744 for the closed loop with and without the DOB, respectively.

5.2.2 Case II: Inverted Pendulum with Backlash

A symmetric backlash with dead-band width of 0.3 (i.e. $\Delta_1 = -\Delta_2 = 0.15$) and slope $K_N = 0.75$ (i.e. 0.25 perturbation in the nominal value) is used. The closed loop response is given in Figs. 9 and 10. The rms values of the tracking error e are 0.0483 and 0.0754 for the closed loop with and without the DOB, respectively.

In both cases $\hat{w}_2$ is obtained in two steps; first the closed loop is run without T_{dist} to get $\hat{w} = \hat{w}_1$, then with T_{dist} to get the overall estimate $\hat{w}$. Then from (23) $\hat{w}_2 = \hat{w} - \hat{w}_1$. Clearly, the closed loop tracking performance is improved with the DOB which rejects the effects of the backlash as well as T_{dist}.

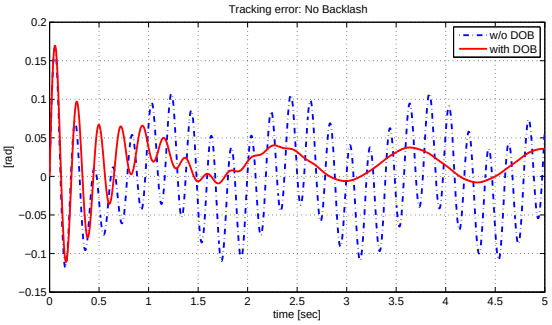

Figure 7. Case I: no backlash; tracking error $e = y_{ref} - y$ with DOB (solid), without DOB (dashed)

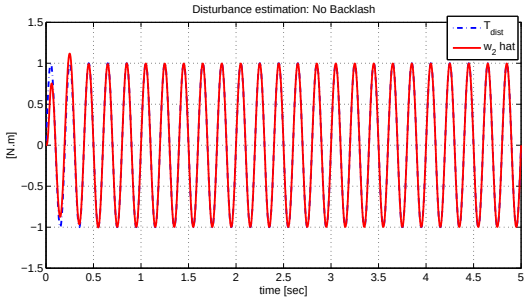

Figure 8. Case I: no backlash; T_{dist} (dash-dot) and $\hat{w}_2$ (solid)

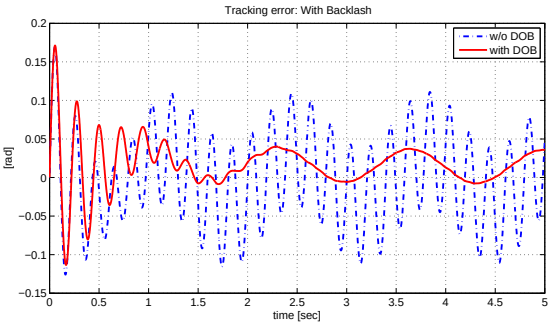

Figure 9. Case II: with backlash; tracking error $e = y_{ref} - y$ with DOB (solid), without DOB (dashed)

6 Conclusions

This paper presented DOB-based control approach to attain robust disturbance rejection and tracking performance in a class of uncertain SISO nonlinear systems. Robustness analysis is studied within the H_∞ framework, and a NLP synthesis approach is subsequently used to obtain a (sub)optimal DOB. Simulation results of an inverted pendulum show that closed loop robust tracking performance is indeed achieved using the DOB.

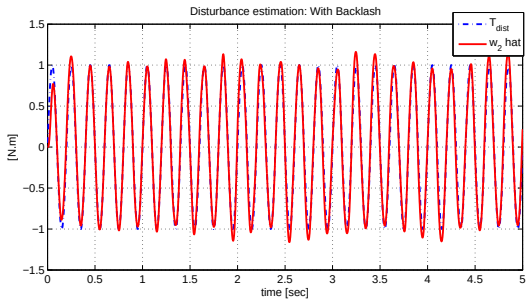

Figure 10. Case II: with backlash; T_{dist} (dash-dot) and $\hat{w}_2$ (solid)

	NLP (fmincon)	SDP	Non-Smooth Syn. (hinfstruct)
$\|W_u T\|_\infty$	0.986	1.41	1.32
$\|W_p (1-Q)\|_\infty$	1.48	1.45	1.14
$\max Re\{\lambda_i\{\tilde{A}-L\tilde{C}\}\}$	-8.4	-7.78	-11.96

Table 1. Optimization Results

REFERENCES

[1] P. Apkarian and D. Noll, Nonsmooth H_∞ Synthesis. IEEE Trans. on Automatic Control, vol. 51(1), pp. 71-86, 2006.

[2] J. Back and H. Shim, Adding Robustness to Nominal Output-Feedback Controllers for Uncertain Nonlinear Systems: a Nonlinear Version of Disturbance Observer. Automatica, vol. 44(10), pp. 2528-2537, 2008.

[3] R. Bickel and M. Tomizuka, Passivity-Based Versus Disturbance Observer Based Robot Control: Equivalence and Stability. ASME Journal of Dynamic Systems, Meas. and Control, vol. 121(1), pp. 41-47, 1999.

[4] N. A. Bruinsma and M. Steinbuch, A Fast Algorithm to Compute the H_∞-norm of a Transfer Function Matrix. Systems and Control Letters, vol. 14(4), pp. 287-293, 1990.

[5] C. Desoer and M. Vidyasagar, Feedback Systems: Input-Output Properties. Academic Press, 1975.

[6] J. Doyle, B. Francis, and A. Tannenbaum. Feedback Control Theory. Macmillan Publishing Co., 1990.

[7] G. E. Dullerud and F. Paganini, A Course in Robust Control Theory. Springer-Verlag, New York, 2000.

[8] R. V. Dwivedula and P. R. Pagillar, Effect of Compliance and Backlash on the Output Speed of a Mechanical Transmission System. ASME Journal of Dynamic Systems, Meas. and Control, vol. 134(3), 2012.

[9] A. H. El-Shaer and T. Zhang, On Robust Distrubance Observer Design Using Semi-Definite Programming. Proc. of the Dynamic Systems Control Conference, Arlington, VA 2011.

[10] A. H. El-Shaer, M. Al Janaideh, P. Krejčí and M. Tomizuka, Robust Performance Enhancement Using Disturbance Observers for Hysteresis Compensation Based on Generalized Prandtl-Ishlinskii Model. Proc. of the American Control Conference, Montreal, QC , pp. 1664 - 1669, 2012.

[11] L. B. Freidovich and H. K. Khalil, Performance Recovery of Feedback-Linearization-Based Designs. IEEE Trans. on Automatic Control, vol. 53(10), pp. 2324-2334, 2008.

[12] P. Gahinet and P. Apkarian, Structured H_∞ Synthesis in MATLAB. Proc. of the 18^{th} IFAC World Congress, Milano, Italy, 2011.

[13] C. D. Johnson, Accommodation of External Disturbances in Linear Regulator and Servomechanism Problems. IEEE Trans. of Automatic Control, vol. 16(6), pp. 635-644, 1971.

[14] H. K. Khalil. Nonlinear Systems. Prentice Hall, 2002.

[15] Matlab Optimization Toolbox, User's Guide R2012b. The MathWorks Inc.

[16] J. Nocedal and S. Wright. Numerical Optimization. Springer, 2006.

[17] M. Nordin and P. -O. Gutman, Controlling Mechanical Systems with Backlash – A Survery. Automatica, vol. 38(10), pp. 1633-1649, 2002.

[18] E. Schrijver and J. V. Dijk, Disturbance Observers for Rigid Mechanical Systems: Equivalence, Stability and Design. ASME Journal of Dynamic Systems, Meas. and Control, vol. 124(4), pp. 539-548, 2002.

[19] R. R. Selmic and F. L. Lewis, Backlash compensation in nonlinear systems using dynamic inversion by neural networks. Proc. of the IEEE Intl. Conference on Control Applications, Kohala Coast, HI, pp. 1163 - 1168, 1999.

[20] S. Shahruz, Performance Enhancement of a Class of Nonlinear Systems by Disturbance Observers. IEEE/ASME Trans. on Mechatronics, vol. 5(3), pp. 319-323, 2000.

[21] S. Shahruz, Suppression of Effects of Nonlinearities by Disturbance Observers. Proc. of the American Control Conference, Boston, Massachusetts, pp. 4342 - 4347, 2004.

[22] D. Söffker, Tie-Jun Yu and P. C. Müller, State Estimation of Dynamical Systems with Nonlinearities by Using Proportional-Integral Observer. Internation Journal of Systems Science, vol. 26(9), 1571-1582, 1995.

[23] T. Umeno, T. Kaneko and Y. Hori. Robust Servosystem Design with Two Degrees of Freedom and its Application to Novel Motion Control of Robot Manipulators. IEEE Trans. on Industrial Elec., vol. 40(5), pp. 473 - 485, 1993.